Increased Nonstationarity of Stormflow Threshold Behaviors in a Forested Watershed Due to Abrupt Earthquake Disturbance

Guotao Zhang[1], Peng Cui[1,2], Carlo Gualtieri [3], Nazir Ahmed Bazai[2], Xueqin Zhang[1], Zhengtao Zhang[4]

[1] Key Laboratory of Land Surface Pattern and Simulation, Institute of Geographic Sciences and Natural Resources Research, Chinese Academy of Sciences, Beijing 100101, China
[2] China-Pakistan Joint Research Center on Earth Sciences, Chinese Academy of Sciences and Higher Education Commission, Islamabad 45320, Pakistan
[3] University of Napoli Federico II, 80125 Napoli, Italy
[4] The Key Laboratory of Environmental Change and Natural Disaster, Ministry of Education, Beijing Normal University, Beijing 100875, China

Correspondence to: Peng Cui (pengcui@imde.ac.cn)

Abstract. Extreme earthquake disturbances to local and regional landscape vegetation could swiftly impair former hydrologic functioning, significantly increasing the challenge of predicting threshold behaviors of rainfall-runoff processes as well as the hydrologic system's complexity over time. It is still unclear how alternating catchment hydrologic behaviors under an ongoing large earthquake disruption are mediated by long-term interactions of landslides and vegetation evolutions. In a famous Wenchuan earthquake-affected watershed, the nonlinear hydrologic behavior is examined as having two thresholds with intervening linear segments. A lower *rising threshold* (TH_r) value (210.48 mm) observed in post-earthquake local landslide regions exhibited a faster response rate of stormflow ~~response faster~~ than that in undisturbed forest and grass-shrub regions, easily triggering huge flash flood disasters. Additionally, an integrated response metric pair (integrated watershed average *generation threshold $TH_{g\text{-}IWA}$* and *rising threshold $TH_{r\text{-}IWA}$*) with areas of disparate land use, ecology, and physiography was proposed and efficiently applied to identify catchment hydrologic emergent behaviors. The interannual variations of two integrated hydrologic thresholds pre- and post-earthquake were assessed to detect the temporal nonstationarity in hydrologic extremes and nonlinear runoff response. The year 2011 was an important turning ~~time~~point along the hydrologic disturbance-recovery timescale~~ following the earthquake~~ ~~in the unsteady recovery process~~, as post-earthquake landslides evolutions reached a state of extreme heterogeneity in space. At that time, the $TH_{r\text{-}IWA}$ value decreased by ~ 9 mm compared to the pre-earthquake level. This is closely related to the fast expansion of landslides leading to a larger extension of variable source area from channel to neighboring hillslopes and faster subsurface stormflow contributing to flash floods. Finally, we present a conceptual model interpreting how the short- and long-term interactions of earthquake-induced landslides and vegetation affect flood hydrographs at event timescale that generated an increased nonstationary hydrologic behavior. This study expands our current knowledge about threshold-based hydrological and nonstationary stormflow behaviors in response to abrupt earthquake disturbance for the prediction of future flood regimes.

1 Introduction

~~Appropriately u~~Understanding and measuring the hydrological processes from local runoff generation mechanisms to larger watershed scales is difficult due to their complexity and nonlinearity (Farrick and Branfireun, 2014;Ross et al., 2021;Scaife et al., 2020). Previous researchers made some efforts to identify the integrated, physically-based hydrologic processes of the rainfall-runoff relationship to predict and simulate catchment runoff behavior under different conditions (Gutierrez-Jurado et al., 2021;Fu et al., 2013b). However, it cannot be generally applied due to uncertainties about water cycle processes, climate inputs, and complex physiographic boundary conditions. The observed hillslope- or catchment-scale threshold runoff response ~~(Zehe and Sivapalan, 2009;Fu et al., 2013a;Ross et al., 2021;Wang et al., 2022)~~ shows a hydrologic emergent pattern (Zehe and Sivapalan, 2009;Fu et al., 2013a;Ross et al., 2021;Wang et al., 2022), which could be used to identify key hydrologic signatures across different spatiotemporal scales (Ali et al., 2013). The hydrologic threshold is the critical point in time or space at which abrupt change in stormflow response occurs (Ali et al., 2013). Below the hydrologic threshold, a small stormflow enters the adjacent channel, but significantly higher runoff magnitudes ~~generally~~ are generally observed above the threshold (Tromp-van Meerveld and McDonnell, 2006;Zehe et al., 2007;Wei et al., 2020). A unified threshold-based hydrological theory that possibly advanced catchment hydrology was extensively discussed during AGU 2011 Fall Meeting (Ali et al., 2013), and later was continuously developed (Ross et al., 2021;Ross, 2021;Ali et al., 2015;Scaife et al., 2020). Theoretical advancements in hydrology can support the development of appropriate algorithms for more efficient predictive hydrologic models.(Ross et al., 2021)

The process of threshold behavior generally shows different nonlinear shapes of hydrological response for a storage-discharge relationship (Ali et al., 2013;Wang et al., 2022), such as the Hockey stick, Step or Heaviside function, Dirac function, and Sigmoid function. The transition from below-threshold to above-threshold behavior for different diagnostic shapes suggests several mechanisms of water retention and release in the watershed. In the literature, the runoff behaviors with Hockey stick shape were found at the hillslope (Tromp-van Meerveld and McDonnell, 2006;Fu et al., 2013a;Wang et al., 2022) and watershed scales (Wei et al., 2020;Scaife et al., 2020;Farrick and Branfireun, 2014) ~~(Wei et al., 2020;Farrick and Branfireun, 2014;Scaife and Band, 2017;Buttle et al., 2019;Zhang et al., 2021a)~~. For example, Farrick and Branfireun (2014) identified a threshold value of 289 mm of gross precipitation (*P*) and antecedent soil water index (*ASI*) in a forested catchment of 3.15 km^2 in Mexico, which presented the threshold behaviors with two-linear runoff response controlled by subsurface stormflow mechanism. While it seemed to follow the Hockey stick shape, above-threshold's stormflow amounts showed high variability (Scaife and Band, 2017;Zhang et al., 2021a). The phenomenon possibly increased the uncertainty of prediction for higher stormflow amounts and flood disasters. Wei et al. (2020) proposed a rainfall-runoff relationship as having multiple thresholds with intervening linear segments to reflect the initial streamflow activation and larger flood response. Understanding the change from slow to rapid stormflow response and larger flash flood hydrograph is vital. However, a clear picture of the physical connotations of threshold behaviors associated with the generation and development of flash flooding is still missing (Wei et al., 2020).

Hydrologic threshold signatures at the catchment scale, as a new diagnostic tool, can effectively evaluate the long-term variations in stormflow response to forest recovery following natural disturbances (Wei et al., 2020;Ali et al., 2013;Scaife and Band, 2017). Natural disturbances in hydrology and associated effects are summarized in Table 1 and categorized into acute disturbances (AD) and chronic disturbances (CD). Acute disturbances, which are abrupt or sudden, such as earthquakes, wildfires, snow and ice, volcanic activity, etc. (Table 1), tend to trigger the most drastic hydrological response and alter the hydrological regime after the disturbance. Comparatively, chronic disturbances (Table 1), which are more gradual and mostly affected by climate change (Hwang et al., 2018;Scaife and Band, 2017;John et al., 2022;Seidl et al., 2017), generally lead to a progressive reduction in forest canopy without immediate destruction of soil-root system and bedrock (Bladon et al., 2019;Hoek Van Dijke et al., 2022). Abrupt disturbance events could significantly alter the original landscape configuration and structure as well as the vegetation-soil system (Figure 1), readily resulting in high peak flows and catastrophic flash flood disasters (Arheimer and Lindström, 2019;Hoek Van Dijke et al., 2022). For instance, the famous Wenchuan earthquake on 12 May 2008 triggered nearly 2.0×10^5 ~~numerous~~ coseismic landslides ~~of nearly 2.0×10⁵~~ (Fan et al., 2018;Xu et al., 2013), leading to the rapid and widespread destruction of vegetation-soil structure and fragment rock mass structures (Cui et al., 2012;Zhang et al., 2021b). These disruptions can reduce the canopy interception and shallow soil water storage capacity, increasing more throughfall precipitation reaching the soil surface and ~~subsurface~~ stormflow magnitudes contributing to the flash flood hydrograph (Zhang et al., 2018). After the abrupt disturbance, the exposed bedrock in the trailing edge of the landslides easily induced the ~~Horton~~Hortonian overland flow, and the generated loose deposition with high soil conductivities in the lower part of the landslides generally increased subsurface stormflow with the microporous flow (Mirus et al., 2017b;Zhang et al., 2018). Such hydrological behaviors are related to the quick runoff generation mechanism with a short lag time, resulting in higher runoff potential (Figure 1). However, the hydrological signature (e.g, soil water movement and stormflow generation) of risky landslides within steep hillslopes was not easy to capture. During the recovery processes, the earthquake-derived amounts of geohazards affected by large rainstorms led to unstable forest shrinkages and landslide expansions ~~(Figure 1)~~ at long-term timescales in a forest-dominated mountainous watershed (Figure 1). The unstable disturbances from endogenous (earthquake) and exogenous (rainstorms and concomitant hydro-geohazards) origins remarkably increased the uncertainty in the assessment of the hydrological regime from disturbance to recovery and flood risk management (Seidl et al., 2017). Previous studies have suffered from over-calibrated hydrological models (Tunas et al., 2020;Maina and Siirila-Woodburn, 2019;Chiang et al., 2019) and a lack of understanding of runoff generation mechanisms in exploiting the effects of natural disturbance events on streamflow response. The efficient identification of nonlinear hydrologic behaviors in an earthquake-affected watershed as well as the understanding of post-earthquake long-term dynamics of hydrologic threshold patterns is still urgently needed.

Table 1: Category and Summary of Natural Disturbances in Hydrology and Associated Effects

Disturbance Agent	Category	Location	Method	Disturbance effects	References
Insect infestation	CD	Oregon in the USA	Field monitoring	Interception, streamflow, evapotranspiration, energy balance	Bladon et al. (2019)

Drought		Rocky Mountain in the USA Colorado in the USA	Remote sensing; Field monitoring and laboratory measurements	Flow path, stream chemistry, peak flow, forest productivity	Knowles et al. (2017); Murphy et al. (2018)
Invasive species		Colorado in the USA	Field monitoring	Water resources, interception, soil intention	Brantley et al. (2013)
Peatland degradation		Finland	Field measurements	Streamflow, water table, stream chemistry	Menberu et al. (2016); Shuttleworth et al. (2019)
Snow and ice		Guangdong in China	Field monitoring	Interception, peak flow	Wei et al. (2020)
Wildfire		Colorado in the USA	Numerical Modeling, Field monitoring and laboratory measurements	Infiltration, interception, erosion, sediment yield, water quality, peak flow	Moody et al. (2013); Ebel (2020)
Volcanic activity	AD	Mount St. Helens in Washington; Patagonia in Chile	Field monitoring and laboratory measurements	Sediment yield, infiltration, runoff, peak flow	Major and Mark (2006); Pierson et al. (2013)
Typhoon		Tacloban in Philippines	Field monitoring and laboratory measurements	Landslides, interceptions, peak flow	Zhang et al. (2018);
Earthquakes		Taiwan in China, Indonesia Sichuan Province in China	Numerical Modeling, Remote sensing, Field monitoring	Landslides, sediment yield, interceptions, peak flow, groundwater level, baseflow	Montgomery and Manga (2003); Tunas et al. (2020); This study

95 *Notes:* CD and AD are chronic disturbance and acute disturbance, respectively.
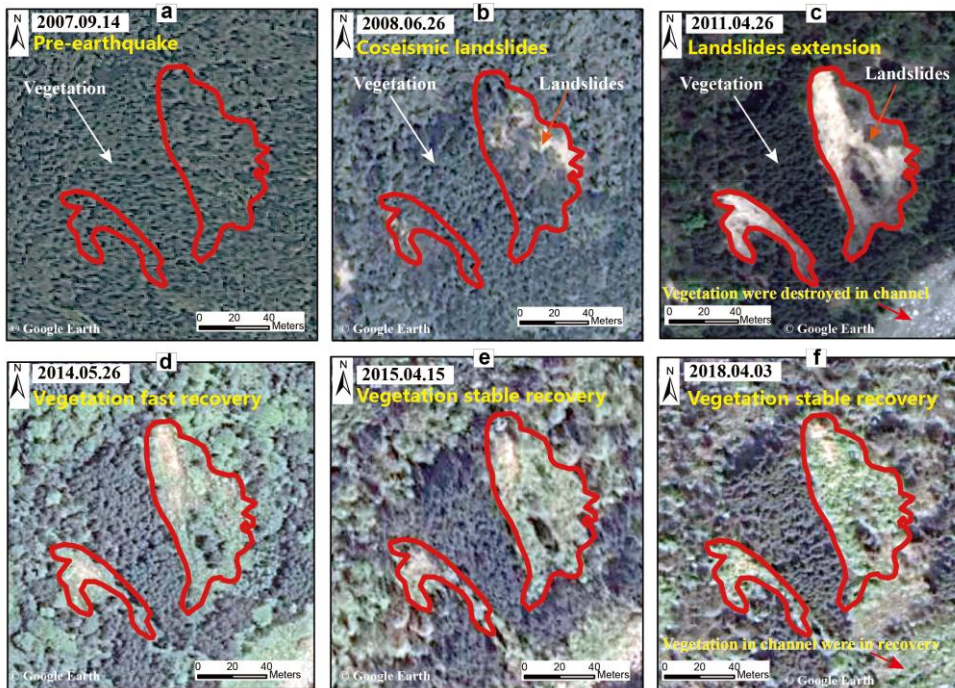
Figure 1: Long-term evolutions of landslides in a disturbed watershed pre- and post-Wenchuan earthquake disturbance.

Additionally, the scarcity of long-term hydrometeorological observation data as well as the inaccessibility of post-earthquake roads is a limitation to understanding the flood response driven by acute disturbance. In this study, the relationship between
100   antecedent soil water storage, rainfall, and runoff at a 5-min interval in an earthquake-affected watershed was investigated. To understand the long-term variations in the hydrologic regime affected by an earthquake and their dominant controls, the intergarted hydrologic thresholds of precipitation + antecedent soil moisture with areas of disparate land use, ecology, and physiography were proposed at the watershed scale. The specific objectives of this study are: (1) to examine the heterogeneity in hydrologic thresholds in undisturbed and disturbed lands; (2) to identify how the subsurface stormflow and variable source
105   area affected by the earthquake-induced landslides control heterogeneity in the non-linear physical processes from rainfall to runoff at the watershed scale; and (3) use of integrated threshold behaviors and linear runoff response to gain insight into the long-term dynamics and nonstationarity of hydrological behaviors affected by the interactions of post-earthquake landslides and vegetations evolution. Assessment of streamflow regime and flood risk at a watershed affected by large physical

disturbances could benefit from the effectively identifying the hydrological threshold signatures that mainly affect a
110   watershed's streamflow response (Ali et al., 2013;Zhang et al., 2021a;Ross et al., 2021).

2 Data and methods

2.1 Study area

This study was carried out in a 78.3 km^2 forested Longxi River (LXR) Experiment Watershed, eastern Tibet Plateau, China
(Figure 2). The forest land occupied 96.9% of the whole watershed area before the 2008 Wenchuan earthquake (Zhang et al.,
115   2021b), mainly consisting of *canopy conifer, dark coniferous,* and *broad-leaf forests.* After the earthquake, the forest land had
a 19.9% shrinkage percentage (Zhang et al., 2021b). The post-earthquake hydro-geohazards, such as landslides and debris
flows, could lead to an unstable recovery trend of landscape vegetation (Figure 1), significantly influencing the stability of
hydrologic function and stormflow behaviors of the watershed from rainfall to runoff (Zhang et al., 2021b).
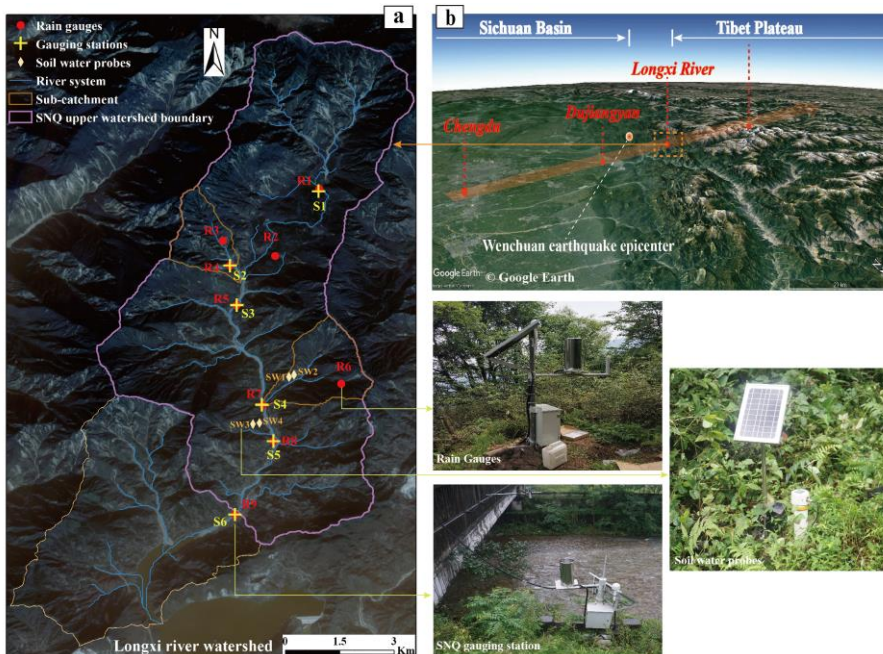
Figure 2: Longxi River (LXR) watershed (78.3 km^2) located in the eastern margin of the Tibet Plateau (**a-b**), affected by the 2008 Wenchuan earthquake, and the detailed monitoring stations, mainly comprising rain gauges (R1-R9), gauging stations (S1-S6) and soil water probes (SW1-SW4).

The soil types mainly consist of Haplic Luvisols, Chromic Luvisols, Dystric Cambisols, and Haplic Alisols. Surface soil hydraulic conductivity in forest land is high, with values of 10-200 mm/h (Zhang et al., 2021a). Subsurface stormflow generated on the soil-bedrock interface under heavy rainfall conditions is a dominant runoff sources contributing to flash flooding (Zhang et al., 2021a). The elevation in the region ranges from 870 to 3284 m asl with high relief. The strong orographic effect generally leads to more rainfall amounts in steep mountainous watersheds (Figure 2b), readily leading to large flood disasters. In the earthquake-affected regions, analyzing the disturbance-recovery processes of landscape vegetation will contribute to understanding potential long-term evolutions in mechanisms of runoff generation and flash flood disasters.

2.2 Hydrometric observations

Open field precipitation from nine rain gauges was automatically recorded at a 5-min interval (Figure 2a), and the flow discharge with high flow velocity and water level during the flood hydrograph was monitored at a 5-min interval and calculated based on the hydraulic Entropy's method (Chen, 2012;Moramarco et al., 2004;Bahmanpouri et al., 2022;Zhang et al., 2021a). Volumetric soil moisture content *(θ)* was recorded at a 5-min interval using the soil water probes (Zhang et al., 2021a). Each probe equipped with eight sensors at a 10 cm depth interval was installed 80 cm in soil profiles below the surface (Figure 2a). The monitored probes (SW1) and (SW2) at upslope and downslope topographic positions were located in an undisturbed forest and grass-shrub lands, respectively, and SW3 and SW4 were located at a disturbed landslide. The *depth equivalent antecedent soil water index* (*DASI*) at the start of each rainfall event was obtained ~~(Zhang et al., 2021a),~~ (Zhang et al., 2021a). ~~which~~ It ~~was~~ is indicative of the initial shallow soil water storage (Wei et al., 2020), and is generally ~~.~~ calculated from the eight-layer soil moisture measurements at each soil profile as (Farrick and Branfireun, 2014):

$$DASI = \sum_{i=1}^{n} \theta_i \left(D_i - D_{i-1} \right) \tag{1}$$

where θ_i indicates the average soil content between i and i-1 soil layer, cm^3 cm^{-3}. i =1, 2, 3, 4……n, and n indicates the number of soil layers below the surface for the monitored soil depth of 80 cm. D_i indicates the soil depth at the ith layer (10, 20, 30, 40, 50, 60, 70, and 80 cm, D_0=0). The index is utilized to exploit the effects of antecedent wetness on the magnitude of hydrologic thresholds and emergent behavior at the hillslope and watershed scales.

2.3 Definitions of storm events and hydrologic thresholds

Storms are defined as events with > 4 mm of precipitation, separated by more than 6 h (Farrick and Branfireun, 2014;Penna et al., 2011). A total of 47 events in this experimental watershed were identified during a time period~~s~~ of June ~ August of every

year from 2018 to 2020, possibly filtering out the uncertainty in assessing hydrological behaviors from seasonal variations of

150 the vegetation forest canopy (Hwang et al., 2018). For each event, the stormflow (Q_q) is separated from the flood hydrograph using a proposed two-parameter recursive digital filter method (Eckhardt, 2005;Zhang et al., 2021a). The catchment threshold behaviors between Q_q and the variable of the sum of $DASI$ + event precipitation amounts (P) at each land-use type were quantitatively assessed using *piecewise regression analysis* (*PRA*), and the hydrologic threshold values of the sum of $DASI+P$ and slope parameters from each linear segment of the *PRA* function were calculated (Zhang et al., 2021a;Oswald et al., 2011).

155 The different breakpoints and slope paraments of *PRA* might contribute to understand the broad controls of shifts from slow to fast stormflow response and flash flood disasters (Zhang et al., 2021a;Scaife and Band, 2017;Oswald et al., 2011). Uncertainty in visually assessing hydrological thresholds is typically increased by nonlinear and complex stormflow behaviors (Detty and McGuire, 2010). However, the automatic identification of thresholds and linear slope parameters with a maximum likelihood approach (Muggeo, 2003) could be effective.

160 **2.4 Determination of nonstationarity in pre- and post-earthquake threshold behaviors**

The earthquake-induced landslides can destroy the soil-vegetation system, reducing the water storage of shallow soil and vegetation canopy and leading to the change in hydrologic thresholds of the sum of $DASI+P$ in the distubed land-use type of landslide. The hydrologic threshold in the landslide is different from other undisturbed land-use types in the watershed. Meanwhile, as long-term evolutions and recovery of landslides (Figure 1), the mutual conversions in land-use types further

165 influence the magnitudes in water storage of shallow soil and vegetation canopy in each land-use type, possibly altering the magnitudes in hydrologic threshold of the sum of $DASI+P$ at watershed scale. Herein, Tto clearly understand long-term threshold evolutions and integral hydrologic emergent behaviors variations pre- and post-earthquake at the watershed scale, an *integrated watershed average* (*IWA*) index for the thresholds considering different land-use types was proposed to characterize the watershed stormflow emergent behaviors. The *IWA* index mainly considers the processes of runoff generation

170 in the watershed's underlying surface based on the principle and framework of runoff potential for curve numbers (Deshmukh et al., 2013). The underlying surface mainly comprises the land use types, the shallow watershedwater storage capacity and physical properties in of soils at different locations, and bedrock types. These factors play vital roles in the processes of runoff generation. Another dominant water source of event precipitation amounts in the atmosphere is also taken into account. Therefore, the index is mainly calculate determined from the area contribution ratio of different land use types (R_i), the shallow

175 water storage capacity at different locations ($DASI_i$), and event precipitation amounts (P) as

$$TH_{i-IWA}(x) = \sum_{i=1}^{n} R_i * x_i = \sum_{i=1}^{n} \frac{a_i}{A} * (DASI_i + P) \tag{2}$$

where $DASI_i$ is the initial shallow water storage capacity of the ith land-use type in the underlying surface (mm), P is the event precipitation (mm), x_i is the runoff generation threshold or rising threshold for the ith land-use type (mm), a_i is the area of the ith land use type (km^2), A is the watershed area of the study area (km^2), R_i is the ratio of a_i and A (%), and n is the number of

land use types, $TH_{i\text{-}IWA}(x)$ is an integrated watershed average index for the thresholds at the watershed scale, with areas of disparate land use, ecology, and physiography. Water bodies, building up and roads are assumed to be impermeable, and the initial storage capacity is assumed to be ~~0~~zero. Based on equation (~~1~~2), $TH_{i\text{-}IWA}(x)$ could be calculated to identify and compare the pre-and post-earthquake variations in thresholds behaviors at ~~a~~ the watershed scale, reflecting the integrated watershed hydrological effects under the long-term interaction and development of the post-earthquake vegetation-hydrogeological hazards.

3 Results

3.1 Stormflow Threshold Behaviors

The collected event precipitation amounts (P) from a series of 40 large storm events ($P>10$mm) (Zhang et al., 2021a) showed a great variation from 16.4 to 263.9 mm. At the larger P values, the stormflow amounts (Q_q) generally had a very large variability, which is similar to the study reported by Farrick and Branfireun (2014). ~~Zhang et al. (2021a);(Farrick and Branfireun, 2014),~~ The phenomenon ~~increasing~~ increases the uncertainty in the estimation of the rainfall-runoff relationship. No significant linear statistical relationship between $DASI$ and Q_q was found in all monitored sites ($p>0.05$, $r^2 \leq 0.017$, see our previous research from Zhang et al. (2021a)). Once the $DASI$ was combined with P, a more visually evident nonlinear threshold behavior for the relationship of $DASI+P$ and Q_q ($p<0.001$) was observed with two hydrologic thresholds or breakpoints of each location (Figures 3), i.e., generation threshold (TH_g) and rising threshold (TH_r).

(a) Forest land (undisturbed) **(b)** Grass-shrub land (undisturbed) **(c)** Landslide land (disturbed)
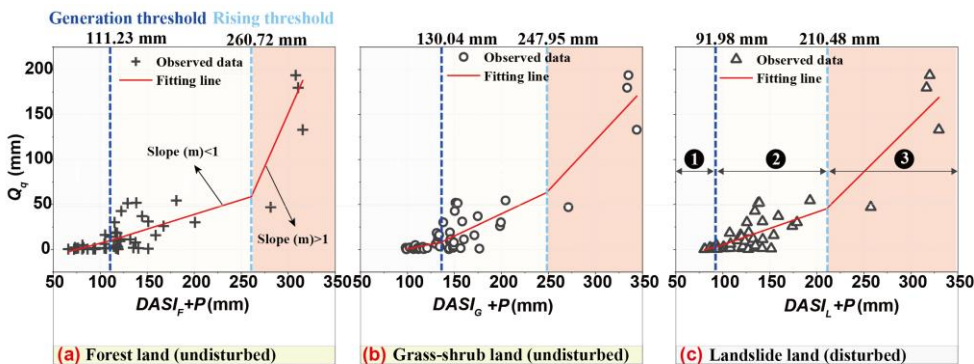
Figure 3: The piecewise regression analysis of event stormflow amount (Q_q) plotted against the sum of event precipitation amounts (P) and $DASI$ at the forest (**a**), grass-shrub (**b**), and landslide (**c**) lands. The undisturbed forest and grass-shrub lands represent the pre-earthquake period, as reported by Zhang et al. (2021a), and the disturbed landslide land represents the post-earthquake period. Redlines indicate the liner fitting for the piecewise regression for the variable of $P+ DASI$ at the confidence level of 95%.

Additionally, significantly lower values in both TH_g (91.98 mm) and TH_r (210.48 mm) were observed in monitored landslide land (Table 2 and Figure 3). The threshold values in TH_g and TH_r in landslide decreased by up to 28.84 mm and 43.86 mm, respectively, compared to those average values in the undisturbed forest and grass-shrub lands. This indicates a lower post-earthquake threshold with response metric pairs that can lead to larger flash flood disasters. The slope parameters from m_{i1} to m_{i3} were different by an order of magnitude (Table 2). A lower value of m_{i1} mainly depicts a more gradual process of runoff generation. Observed larger storms in the third phase readily led to higher m_{i3} values of >1, indicating fast stormflow response during flash flood hydrograph. For different land-use types, lower m_{i3} values occurred in monitored landslide land. It was mainly owing to the deficiency of vegetation canopy and soil water storage capacity, highlighting the contribution of watershed storage during the first and second phases to the abrupt response of flash flooding in the third phase.

Table 2: Comparison of parameters in assessing the three-linear threshold behaviors of $DASI+P$ and Q_q relationships at the confidence level of 95%

Location	Period	Parameters						
		TH_g (mm)	TH_r (mm)	m_{i1}	m_{i2}	m_{i3}	r^2	SEE
Forest land	Pre-earthquake[#]	111.2	260.7	0.28	0.33	2.36	0.88[**]	17.17
Grass-shrub land		130.4	247.9	0.21	0.49	1.12	0.84[**]	15.65
Landslide land	Post-earthquake	91.98	210.48	0.24	0.36	1.04	0.87[**]	16.54

Note:

m_{ij} indicates the values in the slope parameter of PRA equations from the j_{th} phase at the i land (i=forest, grass-shrub, and landslide lands, j=1, 2, 3 shown in Figure 3).

[#] denotes the collected data in a row, reported by Zhang et al. (2021a).

[**] indicates that correlation is significant at the 0.01 level (two-tailed).

SEE is the standard error of estimate in multiple regressions.

3.2 Threshold Pattern Variations at an Earthquake-Affected Watershed

Due to the fragmentation and patchiness of the post-earthquake watershed underlying (Zhang et al., 2021b;Yunus et al., 2020) and unevenness of monitoring locations for different land use (Farrick and Branfireun, 2014), the assessment of the hydrological threshold behavior at the watershed scale is largely uncertain and non-stationary. The scarcity of hydrological information before a large earthquake and road unreachability of post-earthquake disturbed regions increase the difficulty of late monitoring in earthquake-affected watersheds (Mirus et al., 2017a;Zhang et al., 2021a). It limited our knowledge about how the abrupt earthquake affects the stormflow threshold behavior at the watershed scale.

The *integrated watershed average* (*IWA*) index for two thresholds was calculated using equation (12) to characterize the long-term changes in stormflow threshold behaviors pre- and post-earthquake disturbance. Significant lower values in TH_{g-IWA} and

$T\underline{H}_{r\text{-}IWA}$ were found during post-earthquake periods (Figure 4a) and the lowest values (109.34 mm and 250.72 mm) of both occurred in the co-seismic phase. Within 3 years (2008~2011) after the earthquake, the values of both thresholds remain low due to the unstable evolution of post-earthquake hydrogeological hazards (Zhang et al., 2021b;Shen et al., 2020). After the key

230 turning point in 2011 along the hydrological disturbance-recovery process following the earthquake, they recovered rapidly within 3-5 years (2011~2013) after the earthquake and then gradually stabilized and approached the pre-earthquake level. A significant negative correlation relationship ($p<0.05$) between hydrologic thresholds and peak discharges was observed in this experimental watershed (Figure 4b). Shortly after the earthquake, a significantly lower average value with ~9 mm of $T\underline{H}_{r\text{-}IWA}$ at the watershed scale increased peak discharge and event flood volume by up to 22.58% and 25.15%, respectively (Table S1).

235 Figures 4a and b show the variation from 2007 to 2018 in the stormflow threshold behaviors and event flood response. Four phases were observed during the hydrological disturbance-recovery process, effectively and rationally predicting the flood regimes associated with stormflow threshold behaviors due to earthquake disturbance.

带格式的: 正文
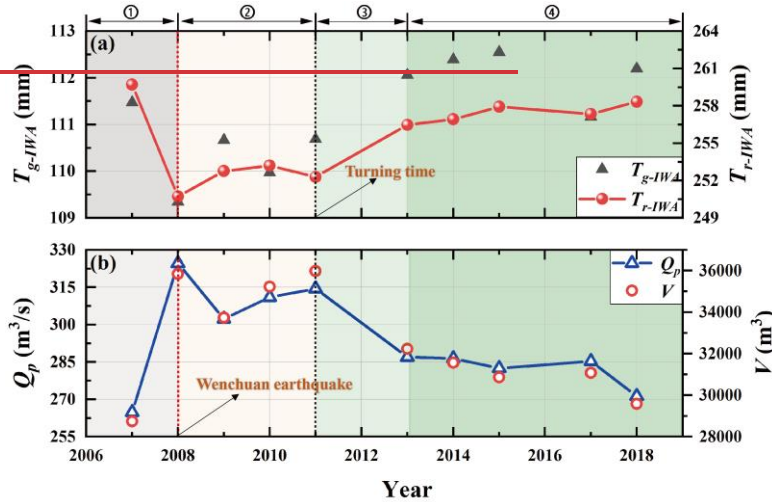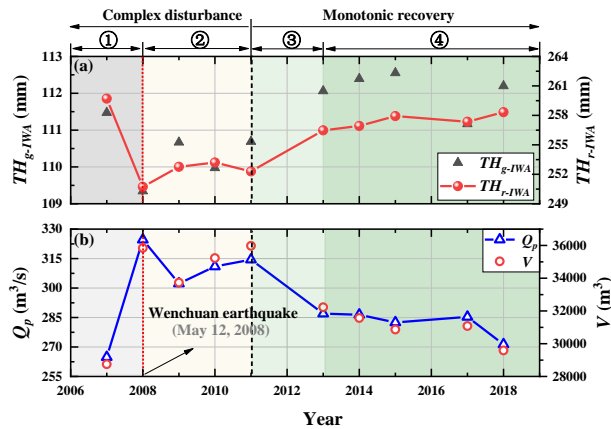
240 **Figure 4:** Changes in (**a**) observed stormflow threshold behaviors, including integrated watershed generation threshold (TH_{g-IWA}) and rising threshold (TH_{r-IWA}), and (**b**) a large flood event response selected from Zhang et al. (2021b) during the periods of 2007 ~ 2018 before and after the earthquake, including peak discharge (Q_p) and event flood volume (V, total flood flow in a single event). ① (2007-2008): TH_{g-IWA} and TH_{r-IWA} abruptly decrease and peak discharge rapidly increases; ② (2008-2011): TH_{g-IWA} and TH_{r-IWA} contain low values triggered by the overlapping of post-earthquake active geohazards; ③ (2011-2013): 245 TH_{g-IWA} and TH_{r-IWA} abruptly increase and peak discharge rapidly decrease; ④ (2013-2018): the hydrologic variables gradually stabilized and approached the pre-earthquake level.

4 Discussion

4.1 Controls on Threshold Behaviors

Those threshold behaviors and nonlinear stormflow responses at the watershed scale are useful for understand the generation 250 and development of flash floods (Zhang et al., 2021a;Wei et al., 2020). They might supplement the threshold-based hydrological theoretical framework (Ali et al., 2013). To extend the application and efficacy of the derived TH_g and TH_r, three large flood events (2019-08-19, 2020-08-15, and 2020-08-29, see Figure 5), with the variation in rainfall intensity (I_{5min}), event accumulative precipitation (EAP) and discharge (Q) at a 5-min interval, were further considered. The TH_g value (120.8 mm) was observed during the rapid streamflow change, and the abrupt change in stormflow and flood response was readily 255 stimulated at the threshold of TH_r with the value of 254.3 mm (Figure 5). Such emergent behavior and signatures at the watershed scale demonstrated the presence of the critical points in time and space where runoff response rapidly changed ~~(Ali et al., 2013;Zhang et al., 2021a)~~. The threshold index was efficiently verified through the applications of the magnitudes in two threshold values during the flood hydrograph (Figure 5) and their concomitant hydrological variations with the discharges derived from runoff potential (Figure 4). However, we also acknowledge a limitation that only the dominant hydrological 260 process of runoff generation was considered while the important hydrological process of ~~confluence~~ flow concentration was

mostly ignored. In a future study, such metrics will be involved in ~~the~~ two hydrological processes of runoff generation and ~~confluence~~ flow concentration to more efficiently reflect the watershed's hydrologic behavior.
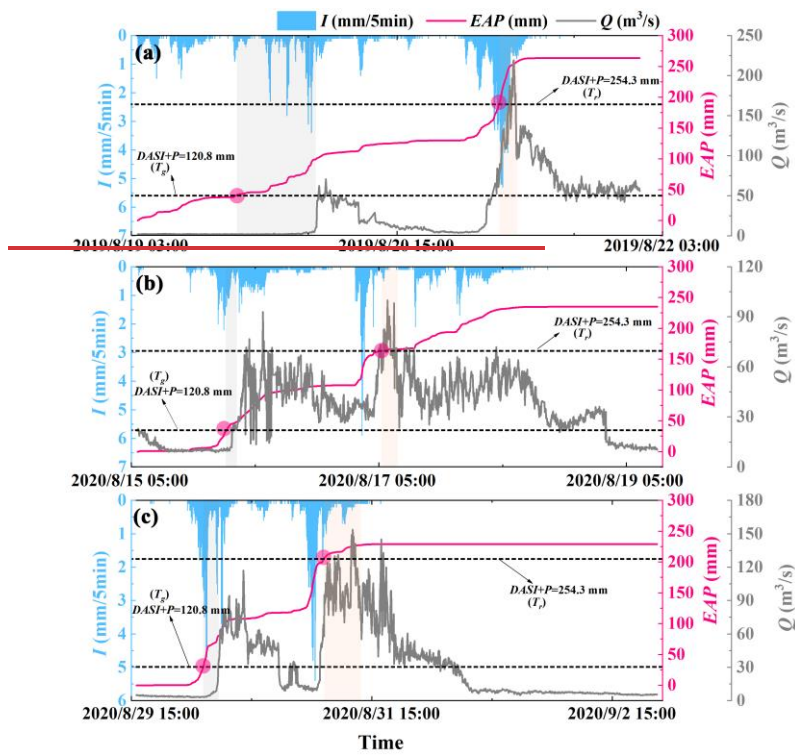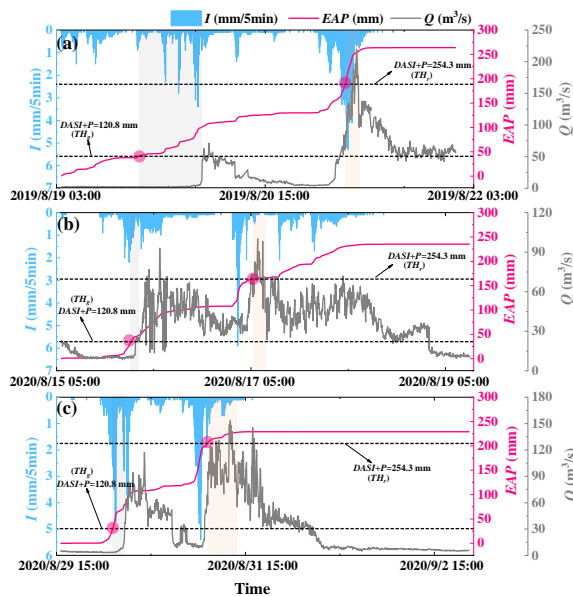
Figure 5: Generation and development of the flash flood hydrograph (**a:** 2019-08-19 event, **b:** 2020-08-15 event, **c:** 2020-08-29 event) with the variation in 5-min rainfall intensity (I_{5min}), event accumulative precipitation (*EAP*), and flow discharge (*Q*) based on the derived generation threshold (*TH_g*) and rising threshold (*TH_r*).

The nonlinear shape of storage-discharge relationships could reflect the runoff-generating mechanisms underlying the retention-release processes of event water input at the watershed scale (Kirchner, 2009;Ali et al., 2013), efficiently diagnosing the inherent change in watershed nonlinear hydrologic behavior. Above the critical threshold value, a rapid discharge response could be significantly observed in Figure 3. ~~It has been demonstrated that~~The bedrock depression storage ~~in~~ on the soil-bedrock interface (Fu et al., 2013b;McDonnell et al., 2021) and antecedent soil moisture storage ~~deficit~~ (Cain et al., 2022;Zhang et al., 2021a;Fu et al., 2013a) are ~~as~~ the main factors controlling the magnitude of ~~initial emergent behavior and~~ the generation threshold (*TH_g*), influencing the~~properties (*T_g*) of rainfall-runoff.~~ initial emergent behavior of rainfall-runoff process. Some common characteristics associated with process-based interpretation are highly permeable soils and low permeability of bedrock at the hillslope with steep slopes (Tromp-van Meerveld and McDonnell, 2006;Farrick and Branfireun, 2014;Scaife and Band, 2017;Ross et al., 2021). These properties generally lead to a significant soil-rock interface, readily triggering the subsurface stormflow on the interface under heavy rainfall conditions. Below and above the generation and rising thresholds, the changes stormflow discharge (*Q_g*, with mean values of 3.14 mm, 22.5 mm, and 138.3 mm, respectively) are significant (Zhang et al., 2021a;Dickinson and Whiteley, 1970). At the *TH_g* value ~~(120.8 mm)~~, the bedrock depressions on the hillslope

could be filled with water from rapid rainfall infiltration while water spilled over the undulating soil-bedrock interface (Figure 6a-b) and generated higher streamflow (Figure 6c). The subsurface stormflow and partly saturated areas (i.e., variable source area) were initially connected to the channel under cumulative rainfall conditions (Farrick and Branfireun, 2015), improving the connectivity of stream-adjacent hillslope hydrological processes and activating the higher streamflow (Figure 6b-c). Once above the T_r value, the variable source areas (*VSA*) close to the channel or impermeable surface under high rainfall intensity showed a significant expansion (Figure 6d). Below and above the generation and rising thresholds, the changes in minimum contributing area (*MCA*, with mean values of 13.79 km², 22.52 km², and 34.43 km², respectively) and stormflow discharge (*Q$_q$*, with mean values of 3.14 mm, 22.5 mm, and 138.3 mm, respectively) are significant (Zhang et al., 2021a;Dickinson and Whiteley, 1970). Higher values of *MCA* above the rising threshold exceeded 60% of the watershed area (Zhang et al., 2021a), It will significantly increasing increase the hydrological connectivity of hillslope riparian-stream and readily facilitating the occurrence of catastrophic flash flood disasters (Figure 6e-f). The abrupt flow process was mainly affected by subsurface stormflow and HortonHortonian overland flow generations at the foot of the slope subjected to storm size and intensity rather than antecedent soil moisture (Zhang et al., 2021a;Farrick and Branfireun, 2014).

295
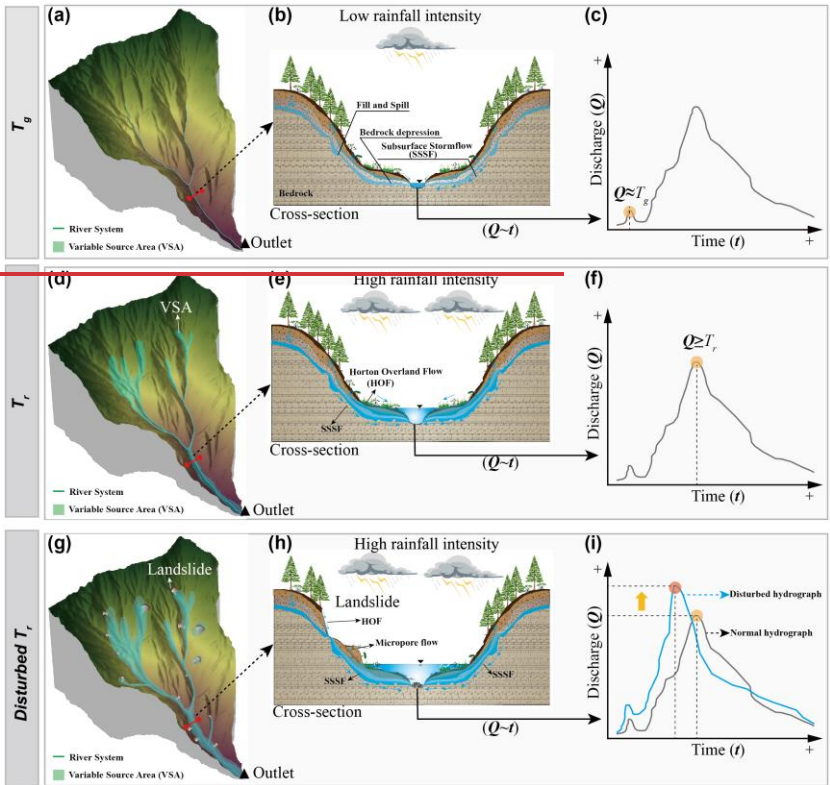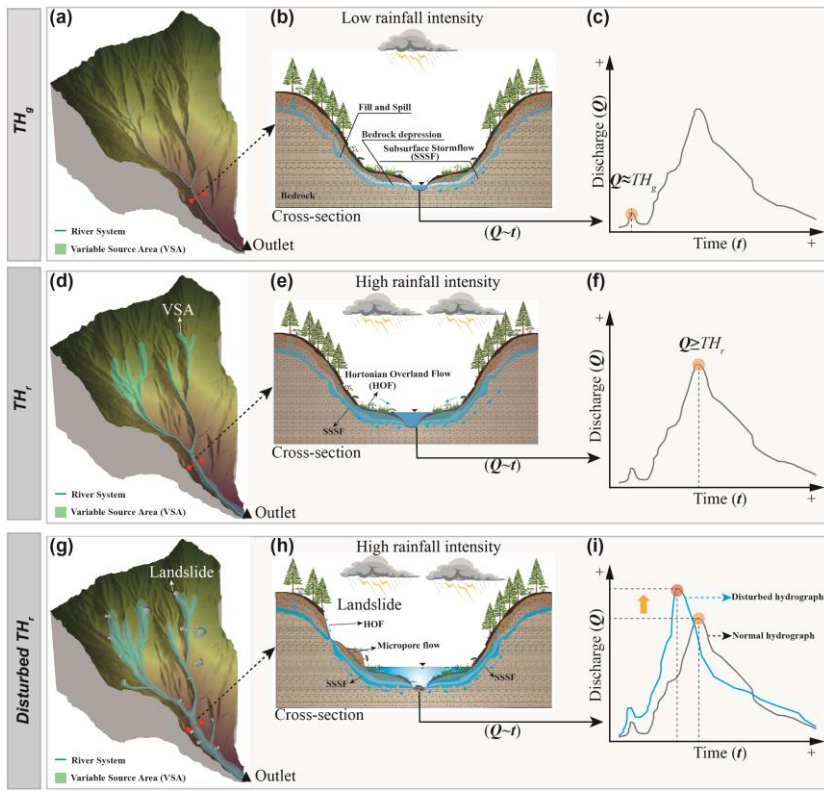
Figure 6: Schematic diagram showing the changes in watershed variable source area (a, d, g), hillslope runoff process at the cross-sections (b, e, h), and flow discharge hydrographs (c, f, i) at the generation threshold (TH_g), rising threshold (TH_r), and TH_r by affected by the earthquake-induced landslides, respectively.

Figure 6g shows the large expansion of *VSA* related to landslides which generally destroy the crown canopy, litter layer, and
300 root-soil system in hillslopes~~(Chiang et al., 2019;Zhang et al., 2021b)~~. These destructive processes alter the original landscape, with the formation of bare rock with steep slopes and accumulations of loose materials (Chiang et al., 2019;Zhang et al., 2021b). For instance, the Wenchuan earthquake-induced ~ 2.0×10^5 landslides decreased by ~30% the forest coverage (Cui et al., 2012), altering the infiltration runoff processes and the contribution of ~~Horton~~Hortonian overland flow flow from the exposed bedrock in the trailing edge of the landslide and subsurface stormflow from landslide-generated loose deposition to flood hydrograph
305 in the channel (Hong et al., 2010;Ran et al., 2015;Sidle et al., 2017) (Figure 6h). Zhang et al. (2021b) applied hydrological model and field observations to demonstrate that the landslides-induced bare land can increase by >10% of the runoff potential

at the watershed scales if compared to that before thepre- earthquake. Peak discharges increased by 22.58%~367.42% and the time to peak was advanced by 25 min. This is almost consistent with Tunas et al. (2020) in the Bangga River Basin affected by the 2018 Palu Earthquake in Indonesia. The large physical disturbances triggered by earthquake-induced landslides can efficiently reflect the reduced water storage of shallow soil and vegetation canopy. The post-disturbance stormflow thresholds of $DASI+P$ can show a lower value (Table 2), and require less water input into the underlying surface to activate the runoff generation and flash flooding.

4.2 Nonstationary Hydrological Behaviors Triggered by Earthquake

Strong earthquake-induced landslides can severely fragmentize original landscape ecosystem but with spatially uneven distribution characteristics, such as the back-slope effect (Wang et al., 2019;Xu et al., 2011;Zhang et al., 2021b), hanging wall effect (Huang and Li, 2009;Beyen, 2019), distance effect along the earthquake fault zone (Xu et al., 2011), etc. These spatially unbalanced conditions generally led to apparent uncertainty and non-stationarity in hydrologic response and runoff generation in the earthquake-affected regions, severeally affecting the identification and judgment of the formation and development of flash floods. Zhang et al. (2021b) first illustrated the change in runoff response on both sides of the Longxi River watershed due to the back-slope effect. They found that the landslide area density of 13.76% on the right bank during the coseismic period was approximately three times that (4.84%) on the left bank, exhibiting an undulating but unpredictable disturbance–recovery process. This phenomenon highlighted the importance of spatially uneven distribution and dynamic nonstationarity at timescales of earthquake-induced landslide patches for an accurate assessment of the runoff generation and the dynamic evolution of catastrophic flash flood.

Interannual variations of rainfall-runoff relationships manifest a slow undulating increase in thresholds after the earthquake (Figure 4a), predicting the short- and long-term changes and nonstationarity in stormflow behaviors at long timescales. These long-term, nonunique interannual thresholds indicated that stormflow behaviors at the watershed scale are closely related to catchment geophysical characteristics (Oswald et al., 2011) or climate (Graham and McDonnell, 2010), changing vegetation dynamics (Hwang et al., 2018) as well as natural disaster disturbance (Ebel and Mirus, 2014). Also, at event timescales, greater thresholds (TH_r) generally occurred during wetter growing seasons (Scaife and Band, 2017;Wei et al., 2020). Above the TH_r, the catastrophic flash flood disasters were readily triggered by summer high-intensity convective storms that possibly activate preferential soil flows facilitating greater and faster stormflow generation in the shallow subsurface (Zhang et al., 2021a). This is associated with the lateral extension of hillslope-channel hydrological connectivity (Farrick and Branfireun, 2014;Ross et al., 2021), abruptly increasing the VSA at the watershed scale.

335
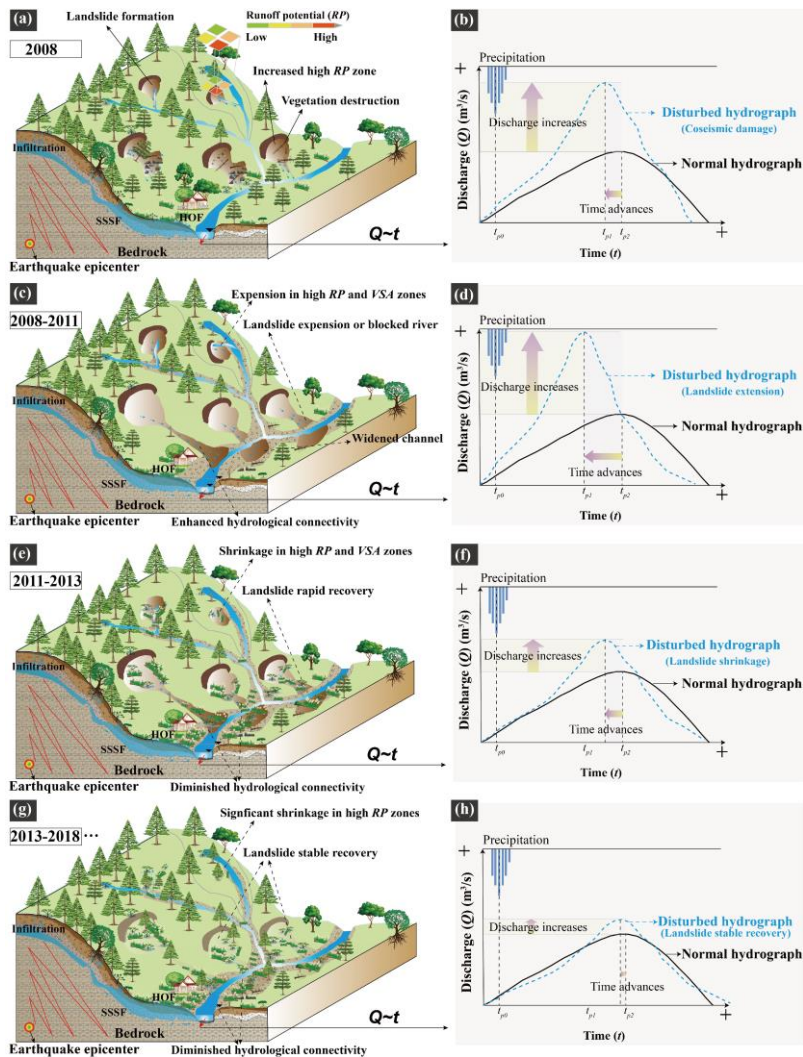
Figure 7: Conceptual model explaining the long-term interactions in disturbed hydrological behaviors during the formation-development-recovery process of the landslides after the Wenchuan earthquake.

By filtering out the influence of climate variables at event timescales, the effects of earthquake disturbance on flash flood hydrographs were evaluated to determine how long-term interactions of earthquake-induced landslides and vegetation might

340 alter interannual stormflow thresholds. Figure 7 presents a conceptual model of the long-term evolution and interaction in disturbed hydrological behaviors, affected by the unsteady formation-development-recovery processes of the landslides after the earthquake. The Wenchuan earthquake largely destroyed the original landscape and vegetation-soil ecosystem triggering hydro-geohazards (Cui et al., 2012;Ran et al., 2015;Shafique, 2020;Zhang et al., 2021b). After the earthquake, the larger landslides with exposed bedrock and loose deposition can lead to more expansion of higher runoff potential (*RP*) and *VSA*

345 zones (Figure 7a). It is related to the ~~Horton~~Hortonian overland flow on exposed bedrock and subsurface stormflow with the microporous flow generated by loose deposition of the landslides. Their processes facilitate quick runoff generation contributing to flood hydrograph. The generation (TH_g) and rising (TH_r) thresholds associated with vegetation canopy interception and antecedent wet conditions ~~(Wei et al., 2020)~~ were significantly lower after the earthquake (Table 2 and Figure 4a), readily leading to a larger flood peak discharge and a shorter time to peak (Figure 7b). Due to the complex geo-hazards

350 processes, the destruction of the vegetation-soil ecosystem and widen channel further expanded the high *RP* and *VSA* zones, and enhanced the structure hydrological connectivity shown in Figure 7c (Moreno-de-las-Heras et al., 2020). The value in TH_r related to the large flash floods drastically decreased (Figure 7d), generating higher peak discharge and less lag time. After the key turning point in 2011, the rapid recovery of landslide and vegetation-soil ecosystem was observed from 2011 to 2013 (Figure 7e-f). During the period, the *RP* and *VSA* zones rapidly expanded while the hydrological threshold behaviors were

355 quickly recovered and improved. Our findings emphasize the importance of earthquake-induced landslides and vegetation dynamics on event- and long-term scale stormflow response, but more research is required to fully understand the disturbed hydrological behaviors and threshold-based hydrological theoretical framework.

4.3 Challenges in Identifying Nonunique Threshold Behaviors disturbed by Large Disaster Events

Abrupt disturbance events generally disrupt the hydrologic storage and functional connectivity at spatial and temporal scales

360 (Ebel and Mirus, 2014), readily leading to the nonunique thresholds in nonlinear behaviors of rainfall-runoff processes (Arheimer and Lindström, 2019;Scaife and Band, 2017). Uncertainties and challenges in characterizing the nonunique threshold behaviors from disturbance hydrology perspectives still need to be clarified.

(1) The lack of detailed observation data about hydrologic fluxes and subsurface storage dynamics before and after an abrupt event is a significant limitation to understanding the variations in flow pathways and runoff generation mechanisms

365 (Farrick and Branfireun, 2014;Ebel, 2020;Chiang et al., 2019). It will be difficult to accurately identify the presence and the form of hydrological threshold signatures that influence a watershed's streamflow response, possibly leading to the assessment uncertainties of the flood hydrologic regime.

(2) The watershed spatially broken patchiness and dispersion brought on by the occurrence of sudden events are very evident (Zhang et al., 2021b;Sidle et al., 2017;Wang et al., 2019), but the methods to quantitatively assess the variable functional

370 hydrologic connectivity associated with runoff generation mechanisms are still lacking (Bracken et al., 2013;Beiter et al.,

2020). This limits our understanding of the sole hydrological responses and variable threshold behaviors by filtering out the effect of loose materials on flooding in the disturbed regions.

(3) Heterogeneity in the regional plant community composition and subsurface critical zone thickness related to water storage capacity (Hahm et al., 2019;Shangguan et al., 2017;García-Gamero et al., 2021) generally leads to different runoff generation mechanisms and nonstationary threshold behaviors in different climate zones. A reasonably generalized ecohydrological zoning with some organizing principles or frameworks could be a better road towards a unified threshold-based hydrology theory proposed by Ali et al. (2013), further facilitating the cross-site syntheses and validation.

5 Conclusions

This study offered insight into the complex interactions of hydrological processes at a small disturbed, forested experimental watershed by revealing relatively simple, generalized nonlinear runoff behaviors. An integrated response metric pair was applied to identify stormflow threshold behaviors and evaluate the long-term threshold dynamics after the Wenchuan earthquake disturbance. Lastly, we revealed the subsurface stormflow and variable source area as dominant controls on the dynamics of threshold behaviors pre- and post-acute disturbance rather than chronic disturbance. Conclusively the key findings mainly are:

(1) Lower values in both generation and rising thresholds derived from nonlinear stormflow behaviors generally occur in disturbed landslide regions, which is easier to lead to large flash flood disasters.

(2) The dynamics of two thresholds through a novel integrated watershed average index can characterize the hydrological disturbance-recovery process before and after an abrupt earthquake.

(3) The runoff generation mechanisms of subsurface stormflow and variable source area mainly control the non-stationarity in threshold behaviors and linear stormflow response. This is related to the largely spatially heterogeneous distribution of abrupt earthquake-induced landslides and temporally undulating recovery of disrupted landscape and vegetation-soil ecosystems. The abrupt hydrological disturbance differs from the nonstationarity in vegetation-climate interactions leading to chronic variable thresholds.

This study emphasizes the importance of integrated stormflow thresholds as a diagnostic tool to effectively characterize abrupt variation in catchment emergent patterns and broad shift from slow to fast flood response, particularly with temporal nonstationarity in long-term interactions of abrupt earthquake-induced landslides and vegetation evolutions. The study contributes to the mitigation and adaptive strategies for unpredictable hydrological regimes and flash flood disasters triggered by abrupt natural disturbances.

Data availability

The data that support the findings of this study are available from the corresponding author upon reasonable request.

Author Contributions

Guotao Zhang: Conceptualization, Methodology, Software, Data curation, Visualization. **Peng Cui:** Conceptualization, Supervision, Funding acquisition, Project administration. **Carlo Gualtieri:** Supervision, Writing – review & editing. **Nazir Ahmed Bazai:** Formal analysis, Writing – review & editing. **Xueqin Zhang:** Funding acquisition, Writing – review & editing. **Zhengtao Zhang:** Software, investigation.

Competing interests

The authors declare that they have no known competing financial interests or personal relationships that could have appeared to influence the work reported in this paper.

Acknowledgments

This study was jointly supported by the Second Tibetan Plateau Scientific Expedition and Research Program (STEP) (Grant No. 2019QZKK0903), National Natural Science Foundation of China (Grant No. U21A2008), the National Natural Science Foundation of China (Grant No. U21A2008 and 42201086), Second Tibetan Plateau Scientific Expedition and Research Program (STEP) (Grant No. 2019QZKK0903), National Natural Science Foundation of China (Grant No. 42201086), National Key R&D Program of China (Grant No. 2022YFC3002902), the National Postdoctoral Program for Innovative Talents (Grant No. BX20220293), the China Postdoctoral Science Foundation (Grant No. 2021M703180), and the Special Research Assistant program of the Chinese Academy of Sciences. We acknowledge the cooperation with Mr. Zhaopeng Song from Insentek Technology Co., Ltd., Hangzhou, China about the support for the Insentek Sensor Probes. Additionally, we are very grateful to the editor (Prof. Genevieve Ali), one public reviewer (Prof. Lawrence Band) and another anonymous reviewer who provided numerous logical comments and constructive suggestions, resulting in an improved manuscript.

References

Ali, G., Oswald, C. J., Spence, C., Cammeraat, E. L. H., McGuire, K. J., Meixner, T., and Reaney, S. M.: Towards a unified threshold-based hydrological theory: necessary components and recurring challenges, Hydrological Processes, 27, 313-318, 10.1002/hyp.9560, 2013.

Ali, G., Tetzlaff, D., McDonnell, J. J., Soulsby, C., Carey, S., Laudon, H., McGuire, K., Buttle, J., Seibert, J., and Shanley, J.: Comparison of threshold hydrologic response across northern catchments, Hydrological Processes, 29, 3575-3591, 10.1002/hyp.10527, 2015.

Arheimer, B., and Lindström, G.: Detecting changes in river flow caused by wildfires, storms, urbanization, regulation, and climate across Sweden, Water Resources Research, 55, 8990-9005, 10.1029/2019WR024759, 2019.

Bahmanpouri, F., Barbetta, S., Gualtieri, C., Ianniruberto, M., Filizola, N., Termini, D., and Moramarco, T.: Prediction of river discharges at confluences based on Entropy theory and surface-velocity measurements, Journal of Hydrology, 606, 127404, https://doi.org/10.1016/j.jhydrol.2021.127404, 2022.

Beiter, D., Weiler, M., and Blume, T.: Characterising hillslope–stream connectivity with a joint event analysis of stream and groundwater levels, Hydrology and Earth System Sciences, 24, 5713-5744, 10.5194/hess-24-5713-2020, 2020.

设置了格式: 英语(英国)

Beyen, K.: Hanging Wall and Footwall Effects in the Largest Reverse-Slip Earthquake of Turkey, October 23, 2011, $${M}_{\mathrm{W}}$$7.2 Van Earthquake, Arabian Journal for Science and Engineering, 44, 4757-4781, 10.1007/s13369-018-3547-x, 2019.

435

Bladon, K. D., Bywater-Reyes, S., LeBoldus, J. M., Kerio, S., Segura, C., Ritokova, G., and Shaw, D. C.: Increased streamflow in catchments affected by a forest disease epidemic, Science of The Total Environment, 691, 112-123, 10.1016/j.scitotenv.2019.07.127, 2019.

Bracken, L. J., Wainwright, J., Ali, G. A., Tetzlaff, D., Smith, M. W., Reaney, S. M., and Roy, A. G.: Concepts of hydrological connectivity: Research approaches, pathways and future agendas, Earth-Science Reviews, 119, 17-34, 10.1016/j.earscirev.2013.02.001, 2013.

440

Brantley, S., Ford, C. R., and Vose, J. M.: Future species composition will affect forest water use after loss of eastern hemlock from southern Appalachian forests, Ecological Applications, 23, 777-790, https://doi.org/10.1890/12-0616.1, 2013.

Buttle, J. M., Webster, K. L., Hazlett, P. W., and Jeffries, D. S.: Quickflow response to forest harvesting and recovery in a northern hardwood forest landscape, Hydrological Processes, 33, 47-65, 10.1002/hyp.13310, 2019.

Cain, M. R., Woo, D. K., Kumar, P., Keefer, L., and Ward, A. S.: Antecedent Conditions Control Thresholds of Tile-Runoff Generation and

445

Nitrogen Export in Intensively Managed Landscapes, Water Resources Research, 58, 10.1029/2021wr030507, 2022.

Chen, Y. C.: Flood discharge measurement of mountain rivers, Hydrology & Earth System Sciences Discussions, 9, 12655-12690, 2012.

Chiang, L.-C., Chuang, Y.-T., and Han, C.-C.: Integrating Landscape Metrics and Hydrologic Modeling to Assess the Impact of Natural Disturbances on Ecohydrological Processes in the Chenyulan Watershed, Taiwan, International journal of environmental research and public health, 16, 266, 10.3390/ijerph16020266, 2019.

450

Cui, P., Lin, Y., and Chen, C.: Destruction of vegetation due to geo-hazards and its environmental impacts in the Wenchuan earthquake areas, Ecological Engineering, 44, 61-69, 10.1016/j.ecoleng.2012.03.012, 2012.

Deshmukh, D. S., Chaube, U. C., Ekube Hailu, A., Aberra Gudeta, D., and Tegene Kassa, M.: Estimation and comparision of curve numbers based on dynamic land use land cover change, observed rainfall-runoff data and land slope, Journal of Hydrology, 492, 89-101, 10.1016/j.jhydrol.2013.04.001, 2013.

455

Detty, J. M., and McGuire, K. J.: Threshold changes in storm runoff generation at a till-mantled headwater catchment, Water Resources Research, 46, 10.1029/2009wr008102, 2010.

Dickinson, W., and Whiteley, H.: Watershed areas contributing to runoff, IAHS publ, 96, 12-26, 1970.

Ebel, B. A., and Mirus, B. B.: Disturbance hydrology: challenges and opportunities, Hydrological Processes, 28, 5140-5148, 10.1002/hyp.10256, 2014.

460

Ebel, B. A.: Temporal evolution of measured and simulated infiltration following wildfire in the Colorado Front Range, USA: Shifting thresholds of runoff generation and hydrologic hazards, Journal of Hydrology, 124765, 2020.

Eckhardt, K.: How to construct recursive digital filters for baseflow separation, Hydrological Processes, 19, 507-515, 10.1002/hyp.5675, 2005.

Fan, X., Juang, C. H., Wasowski, J., Huang, R., Xu, Q., Scaringi, G., van Westen, C. J., and Havenith, H.-B.: What we have learned from

465

the 2008 Wenchuan Earthquake and its aftermath: A decade of research and challenges, Engineering Geology, 241, 25-32, 10.1016/j.enggeo.2018.05.004, 2018.

Farrick, K. K., and Branfireun, B. A.: Soil water storage, rainfall and runoff relationships in a tropical dry forest catchment, Water Resources Research, 50, 9236-9250, 10.1002/2014WR016045, 2014.

Farrick, K. K., and Branfireun, B. A.: Flowpaths, source water contributions and water residence times in a Mexican tropical dry forest

470

catchment, Journal of Hydrology, 529, 854-865, 10.1016/j.jhydrol.2015.08.059, 2015.

Fu, C., Chen, J., Jiang, H., and Dong, L.: Threshold behavior in a fissured granitic catchment in southern China: 1. Analysis of field monitoring results, Water Resources Research, 49, 2519-2535, 10.1002/wrcr.20191, 2013a.

Fu, C., Chen, J., Jiang, H., and Dong, L.: Threshold behavior in a fissured granitic catchment in southern China: 2. Modeling and uncertainty analysis, Water Resources Research, 49, 2536-2551, 10.1002/wrcr.20193, 2013b.

475

García-Gamero, V., Peña, A., Laguna, A. M., Giráldez, J. V., and Vanwalleghem, T.: Factors controlling the asymmetry of soil moisture and vegetation dynamics in a hilly Mediterranean catchment, Journal of Hydrology, 598, 126207, https://doi.org/10.1016/j.jhydrol.2021.126207, 2021.

Graham, C. B., and McDonnell, J. J.: Hillslope threshold response to rainfall: (2) Development and use of a macroscale model, Journal of Hydrology, 393, 77-93, 10.1016/j.jhydrol.2010.03.008, 2010.

480

Gutierrez-Jurado, K. Y., Partington, D., and Shanafield, M.: Taking theory to the field: streamflow generation mechanisms in an intermittent Mediterranean catchment, Hydrology and Earth System Sciences, 25, 4299-4317, 10.5194/hess-25-4299-2021, 2021.

Hahm, W. J., Rempe, D. M., Dralle, D. N., Dawson, T. E., Lovill, S. M., Bryk, A. B., Bish, D. L., Schieber, J., and Dietrich, W. E.: Lithologically Controlled Subsurface Critical Zone Thickness and Water Storage Capacity Determine Regional Plant Community Composition, Water Resources Research, 55, 3028-3055, 10.1029/2018wr023760, 2019.

485

Hoek Van Dijke, A. J., Herold, M., Mallick, K., Benedict, I., Machwitz, M., Schlerf, M., Pranindita, A., Theeuwen, J. J. E., Bastin, J.-F., and Teuling, A. J.: Shifts in regional water availability due to global tree restoration, Nature Geoscience, 15, 363-368, 10.1038/s41561-022-00935-0, 2022.

Hong, N. M., Chu, H. J., Lin, Y. P., and Deng, D. P.: Effects of land cover changes induced by large physical disturbances on hydrological responses in Central Taiwan, Environ Monit Assess, 166, 503-520, 10.1007/s10661-009-1019-1, 2010.

490 Huang, R., and Li, W.: Development and distribution of geohazards triggered by the 5.12 Wenchuan Earthquake in China, Science in China Series E: Technological Sciences, 52, 810-819, 10.1007/s11431-009-0117-1, 2009.

Hwang, T., Martin, K. L., Vose, J. M., Wear, D., Miles, B., Kim, Y., and Band, L. E.: Nonstationary Hydrologic Behavior in Forested Watersheds Is Mediated by Climate-Induced Changes in Growing Season Length and Subsequent Vegetation Growth, Water Resources Research, 54, 5359-5375, 10.1029/2017wr022279, 2018.

495 John, A., Nathan, R., Horne, A., Fowler, K., and Stewardson, M.: Nonstationary Runoff Responses Can Interact With Climate Change to Increase Severe Outcomes for Freshwater Ecology, Water Resources Research, 58, 10.1029/2021wr030192, 2022.

Kirchner, J. W.: Catchments as simple dynamical systems: Catchment characterization, rainfall-runoff modeling, and doing hydrology backward, Water Resources Research, 45, 10.1029/2008wr006912, 2009.

Knowles, J. F., Lestak, L. R., and Molotch, N. P.: On the use of a snow aridity index to predict remotely sensed forest productivity in the
500 presence of bark beetle disturbance, Water Resources Research, 53, 4891-4906, https://doi.org/10.1002/2016WR019887, 2017.

Maina, F. Z., and Siirila-Woodburn, E. R.: Watersheds dynamics following wildfires: Nonlinear feedbacks and implications on hydrologic responses, Hydrological Processes, 34, 33-50, 10.1002/hyp.13568, 2019.

Major, J. J., and Mark, L. E.: Peak flow responses to landscape disturbances caused by the cataclysmic 1980 eruption of Mount St. Helens, Washington, Geological Society of America Bulletin, 118, 938-958, 2006.

505 McDonnell, J. J., Spence, C., Karran, D. J., Ilja van Meerveld, H. J., and Harman, C.: Fill-and-spill: A process description of runoff generation at the scale of the beholder, Water Resources Research, 57, e2020WR027514, 10.1029/2020WR027514, 2021.

Menberu, M. W., Tahvanainen, T., Marttila, H., Irannezhad, M., Ronkanen, A.-K., Penttinen, J., and Kløve, B.: Water-table-dependent hydrological changes following peatland forestry drainage and restoration: Analysis of restoration success, Water Resources Research, 52, 3742-3760, https://doi.org/10.1002/2015WR018578, 2016.

510 Mirus, B. B., Ebel, B. A., Mohr, C. H., and Zegre, N.: Disturbance hydrology: Preparing for an increasingly disturbed future, Water Resources Research, 53, 10007-10016, 2017a.

Mirus, B. B., Smith, J. B., and Baum, R. L.: Hydrologic Impacts of Landslide Disturbances: Implications for Remobilization and Hazard Persistence, Water Resources Research, 53, 8250-8265, 10.1002/2017wr020842, 2017b.

Montgomery, D. R., and Manga, M.: Streamflow and water well responses to earthquakes, Science, 300, 2047-2049,
515 10.1126/science.1082980, 2003.

Moody, J. A., Shakesby, R. A., Robichaud, P. R., Cannon, S. H., and Martin, D. A.: Current research issues related to post-wildfire runoff and erosion processes, Earth-Science Reviews, 122, 10-37, 10.1016/j.earscirev.2013.03.004, 2013.

Moramarco, T., Saltalippi, C., and Singh, V. P.: Estimation of Mean Velocity in Natural Channels Based on Chiu's Velocity Distribution Equation, Journal of Hydrologic Engineering, 9, 42-50, 2004.

520 Moreno-de-las-Heras, M., Merino-Martín, L., Saco, P. M., Espigares, T., Gallart, F., and Nicolau, J. M.: Structural and functional control of surface-patch to hillslope-scale runoff and sediment connectivity in Mediterranean-dry reclaimed slope systems, Hydrology and Earth System Sciences Discussions, 1-28, 2020.

Muggeo, V. M. R.: Estimating regression models with unknown break-points, Statistics in Medicine, 22, 3055-3071, 10.1002/sim.1545, 2003.

525 Murphy, S. F., McCleskey, R. B., Martin, D. A., Writer, J. H., and Ebel, B. A.: Fire, Flood, and Drought: Extreme Climate Events Alter Flow Paths and Stream Chemistry, Journal of Geophysical Research: Biogeosciences, 123, 2513-2526, https://doi.org/10.1029/2017JG004349, 2018.

Oswald, C. J., Richardson, M. C., and Branfireun, B. A.: Water storage dynamics and runoff response of a boreal Shield headwater catchment, Hydrological Processes, 25, 3042-3060, 10.1002/hyp.8036, 2011.

530 Penna, D., Tromp-van Meerveld, H., Gobbi, A., Borga, M., and Dalla Fontana, G.: The influence of soil moisture on threshold runoff generation processes in an alpine headwater catchment, Hydrology and Earth System Sciences, 15, 689-702, 10.5194/hess-15-689-2011, 2011.

Pierson, T. C., Major, J. J., Amigo, Á., and Moreno, H.: Acute sedimentation response to rainfall following the explosive phase of the 2008–2009 eruption of Chaitén volcano, Chile, Bulletin of Volcanology, 75, 723, 10.1007/s00445-013-0723-4, 2013.

535 Ran, Q., Qian, Q., LI, W., Fang, Q., Fu, X., Yu, X., and Yueping, X.: Impact of earthquake-induced-landslides on hydrologic response of a steep mountainous catchment: a case study of the Wenchuan earthquake zone, Journal of Zhejiang University SCIENCE A, 16, 131-142, 10.1631/jzus.A1400039, 2015.

Ross, C. A.: Moving towards a unified threshold-based hydrological theory through inter-comparison and modelling, 2021.

Ross, C. A., Ali, G. A., Spence, C., and Courchesne, F.: Evaluating the Ubiquity of Thresholds in Rainfall-Runoff Response Across
540 Contrasting Environments, Water Resources Research, 57, 10.1029/2020wr027498, 2021.

Scaife, C. I., and Band, L. E.: Nonstationarity in threshold response of stormflow in southern Appalachian headwater catchments, Water Resources Research, 53, 6579-6596, 10.1002/2017wr020376, 2017.

Scaife, C. I., Singh, N. K., Emanuel, R. E., Miniat, C. F., and Band, L. E.: Non-linear quickflow response as indicators of runoff generation mechanisms, Hydrological Processes, 34, 2949-2964, 10.1002/hyp.13780, 2020.

545 Seidl, R., Thom, D., Kautz, M., Martin-Benito, D., Peltoniemi, M., Vacchiano, G., Wild, J., Ascoli, D., Petr, M., Honkaniemi, J., Lexer, M. J., Trotsiuk, V., Mairota, P., Svoboda, M., Fabrika, M., Nagel, T. A., and Reyer, C. P. O.: Forest disturbances under climate change, Nature Climate Change, 7, 395-402, 10.1038/nclimate3303, 2017.

Shafique, M.: Spatial and temporal evolution of co-seismic landslides after the 2005 Kashmir earthquake, Geomorphology, 362, 107228, 10.1016/j.geomorph.2020.107228, 2020.

550 Shangguan, W., Hengl, T., Mendes De Jesus, J., Yuan, H., and Dai, Y.: Mapping the global depth to bedrock for land surface modeling, Journal of Advances in Modeling Earth Systems, 9, 65-88, 10.1002/2016ms000686, 2017.

Shen, P., Zhang, L. M., Fan, R. L., Zhu, H., and Zhang, S.: Declining geohazard activity with vegetation recovery during first ten years after the 2008 Wenchuan earthquake, Geomorphology, 352, 106989, 10.1016/j.geomorph.2019.106989, 2020.

Shuttleworth, E. L., Evans, M. G., Pilkington, M., Spencer, T., Walker, J., Milledge, D., and Allott, T. E. H.: Restoration of blanket peat
555 moorland delays stormflow from hillslopes and reduces peak discharge, Journal of Hydrology X, 2, 100006, https://doi.org/10.1016/j.hydroa.2018.100006, 2019.

Sidle, R. C., Gomi, T., Loaiza Usuga, J. C., and Jarihani, B.: Hydrogeomorphic processes and scaling issues in the continuum from soil pedons to catchments, Earth-Science Reviews, 175, 75-96, 10.1016/j.earscirev.2017.10.010, 2017.

Tromp-van Meerveld, H. J., and McDonnell, J. J.: Threshold relations in subsurface stormflow: 1. A 147-storm analysis of the Panola
560 hillslope, Water Resources Research, 42, 336-336, 10.1029/2004WR003778, 2006.

Tunas, I. G., Tanga, A., and Oktavia, S.: Impact of Landslides Induced by the 2018 Palu Earthquake on Flash Flood in Bangga River Basin, Sulawesi, Indonesia, Journal of Ecological Engineering, 21, 190-200, 10.12911/22998993/116325, 2020.

Wang, J., Jin, W., Cui, Y.-f., Zhang, W.-f., Wu, C.-h., and Alessandro, P.: Earthquake-triggered landslides affecting a UNESCO Natural Site: the 2017 Jiuzhaigou Earthquake in the World National Park, China, Journal of Mountain Science, 15, 1412-1428, 10.1007/s11629-018-
565 4823-7, 2019.

Wang, S., Yan, Y., Fu, Z., and Chen, H.: Rainfall-runoff characteristics and their threshold behaviors on a karst hillslope in a peak-cluster depression region, Journal of Hydrology, 605, 10.1016/j.jhydrol.2021.127370, 2022.

Wei, L., Qiu, Z., Zhou, G., Kinouchi, T., and Liu, Y.: Stormflow threshold behaviour in a subtropical mountainous headwater catchment during forest recovery period, Hydrological Processes, 34, 1728-1740, 10.1002/hyp.13658, 2020.

570 Xu, C., Xu, X., Yao, X., and Dai, F.: Three (nearly) complete inventories of landslides triggered by the May 12, 2008 Wenchuan Mw 7.9 earthquake of China and their spatial distribution statistical analysis, Landslides, 11, 441-461, 10.1007/s10346-013-0404-6, 2013.

Xu, Q., Zhang, S., and Li, W.: Spatial distribution of large-scale landslides induced by the 5.12 Wenchuan Earthquake, Journal of Mountain Science, 8, 246-260, 10.1007/s11629-011-2105-8, 2011.

Yunus, A. P., Fan, X., Tang, X., Jie, D., Xu, Q., and Huang, R.: Decadal vegetation succession from MODIS reveals the spatio-temporal
575 evolution of post-seismic landsliding after the 2008 Wenchuan earthquake, Remote Sensing of Environment, 236, 111476, 10.1016/j.rse.2019.111476, 2020.

Zehe, E., Elsenbeer, H., Lindenmaier, F., Schulz, K., and Blöschl, G.: Patterns of predictability in hydrological threshold systems, Water Resources Research, 43, 10.1029/2006wr005589, 2007.

Zehe, E., and Sivapalan, M.: Threshold behaviour in hydrological systems as (human) geo-ecosystems: manifestations, controls, implications,
580 Hydrology and Earth System Sciences, 13, 1273-1297, 10.5194/hess-13-1273-2009, 2009.

Zhang, G., Cui, P., Gualtieri, C., Zhang, J., Ahmed Bazai, N., Zhang, Z., Wang, J., Tang, J., Chen, R., and Lei, M.: Stormflow generation in a humid forest watershed controlled by antecedent wetness and rainfall amounts, Journal of Hydrology, 603, 127107, https://doi.org/10.1016/j.jhydrol.2021.127107, 2021a.

Zhang, G., Cui, P., Jin, W., Zhang, Z., Wang, H., Bazai, N. A., Li, Y., Liu, D., and Pasuto, A.: Changes in hydrological behaviours triggered
585 by earthquake disturbance in a mountainous watershed, Science of The Total Environment, 760, 143349, 10.1016/j.scitotenv.2020.143349, 2021b.

Zhang, J., van Meerveld, H. J., Tripoli, R., and Bruijnzeel, L. A.: Runoff response and sediment yield of a landslide-affected fire-climax grassland micro-catchment (Leyte, the Philippines) before and after passage of typhoon Haiyan, Journal of Hydrology, 565, 524-537, 10.1016/j.jhydrol.2018.08.016, 2018.

590